Vibronic energies and spectra of molecular dimers

A. Eisfeld, L. Braun, W. T. Strunz, and J. S. Briggs[a]
*Fakultät für Mathematik und Physik, Universität Freiburg, Hermann-Herder-Strasse 3,
D-79104 Freiburg, Germany*

J. Beck and V. Engel
Institut für Physikalische Chemie, Universität Würzburg, Am Hubland, D-97074 Würzburg, Germany

We consider three distinct methods of calculating the vibronic levels and absorption spectra of molecular dimers coupled by dipole-dipole interactions. The first method is direct diagonalization of the vibronic Hamiltonian in a basis of monomer eigenstates. The second method is to use creation and annihilation operators leading in harmonic approximation to the Jaynes–Cummings Hamiltonian. The adiabatic approximation to this problem provides insight into spectral behavior in the weak and strong coupling limits. The third method, which serves as a check on the accuracy of the previous methods, is a numerically exact solution of the time-dependent Schrödinger equation. Using these methods, dimer spectra are calculated for three separate dye molecules and show good agreement with measured spectra. © 2005 American Institute of Physics.
[DOI: 10.1063/1.1861883]

I. INTRODUCTION

The simple molecular dimer is a classic case for the study of the coupling between electronic and vibrational excitation.[1–6] This vibronic coupling has been analyzed extensively in an approximation in which only the electronic ground state and a single electronic excited state are coupled to a single mode of internal vibrational excitation, which is considered to be harmonic in both ground and excited electronic states. In this very simplest approximation the two-state vibronic coupling time-independent Schrödinger equation has been shown to separate into two decoupled equations. One has an analytic solution, being a displaced harmonic oscillator. The other equation was solved numerically by Fulton and Gouterman[3] in 1964, in perhaps the first application of a computer to this problem. This work also made use of a natural measure for coupling strength which had been recognized earlier by Simpson and Peterson[7] in connection with vibronic coupling in the more complicated polymer problem. This measure is the ratio of the electronic (dipole-dipole) coupling strength (which we call J) to an energy (which we call Δ) characteristic of the shift of the equilibrium position on excitation and of the harmonic frequency ω. Up to factors of the order of unity, depending on precise definition, Δ appears as the width of the vibrational absorption spectrum from ground to excited electronic state. Strong coupling then is characterized by $|J/\Delta| \gg 1$ and weak coupling by $|J/\Delta| \ll 1$.

It has, perhaps, not been adequately recognized that the above problem of a two-level system interacting with a single oscillator mode is similar to aspects of the "spin-boson Hamiltonian" problem of solid-state physics[8] and more particularly is *identical* to the Jaynes–Cummings (JC) model[9] of quantum optics. In this latter case a two-level atom interacts

with a quantized (harmonic) radiation field. In the following we will analyze this similarity in more detail, particularly as regards the use of an adiabatic approximation in understanding changes in the dimer spectrum as J/Δ is varied.

We find it illustrative to employ three independent strategies for solution. The first method (1) treats the vibronic problem by an expansion in basis functions which leads to the diagonalization of an algebraic problem whose input are Franck–Condon (FC) factors between ground and excited states. The second method (2) uses operator techniques and is ideally suited to the harmonic case of the JC model and readily allows an adiabatic approximation to be made. The third method (3) is completely different in using the time-dependent rather than time-independent Schrödinger equation. Exploiting modern developments in the numerical time propagation of quantum states, the absorption spectrum can be constructed from the long-time limit. This method has the advantage that arbitrary Born–Oppenheimer (BO) potential functions involve no increase in computer time.

Although exact solutions obtained with all three methods of course yield the same results, hitherto they have been used largely in different fields. Method (1) is the one most used for the calculation of eigenenergies, method (3) mostly for time-dependent molecular problems. Method (2) has found wide use in quantum optics and solid state physics. Differences between the methods appear when approximations are made and each gives insight into different aspects of exact solutions. For example, in method (1) one can include only a limited number of vibrational levels in upper and lower states, then gradually increase this number to see how the spectrum develops. Method (2) lends itself to the adiabatic approximation, which gives direct insight into coupling of electronic levels through the nuclear motion. Method (3) only gives fully resolved eigenenergies when time propagation is many times greater than vibrational periods. Stopping

---

[a]Electronic mail: briggs@physik.uni-freiburg.de

122, 134103-1

the time propagation at intermediate times is equivalent to spectroscopy under low resolution, or can be used to mimic line-broadening effects. However, unlike method (1), method (3) implicitly includes all vibrational levels, including the continuum, in both ground and excited electronic states. Hence we will compare and contrast all three methods below.

The plan of the paper is as follows. In Sec. II we treat the problem in first quantization. In Sec. III, using an operator representation, the harmonic case is considered in some detail. Particular emphasis is given to the adiabatic approximation. In Sec. IV the time-dependent approach is applied. In Sec. V we compare our results to measured dimer spectra and find good agreement. We conclude with a short summary and a discussion of our findings.

II. THE DIMER PROBLEM IN FIRST QUANTIZATION

Our model problem is that of two identical monomers at fixed orientation and separation, interacting via transition dipole-dipole force. Only a single excited electronic state is taken into account. The electronic motion is coupled to intramolecular vibrations (not necessarily harmonic) in both ground and excited states. The approximation will be made that the electronic dipole-dipole coupling matrix element is independent of vibrational coordinates.

A. The monomer

Denoting the electronic and nuclear coordinates of monomer n $(n=1,2)$ with r_n and ρ_n, respectively, the monomer Hamiltonian is given by

$$H_n = H_n^{\text{el}}(r_n,\rho_n) + T_n^{\text{nuc}}(\rho_n) + V_n^{\text{nuc}}(\rho_n), \tag{1}$$

where H_n^{el} is the electronic part of the Hamiltonian which depends parametrically on the nuclear coordinates ρ_n, and T_n^{nuc} and V_n^{nuc} are the monomer kinetic and potential energy, respectively. The time independent Schrödinger equation for the electronic part is

$$H_n^{\text{el}}(r_n,\rho_n)\phi_n^M(r_n,\rho_n) = W_n^M(\rho_n)\phi_n^M(r_n,\rho_n) \tag{2}$$

and has eigenfunctions $\phi_n^M(r_n,\rho_n)$ and eigenenergies $W_n^M(\rho_n)$ that depend also parametrically on ρ_n. Here the index M refers to a particular electronic state. We are only considering one electronic excited state, so we will use $M=g$ for the electronic ground state and $M=e$ for the electronic excited state. In BO approximation we write the eigenfunctions of the monomer Hamiltonian (1) as

$$\phi_n^M(r_n,\rho_n)\xi_{nM}^\alpha(\rho_n), \tag{3}$$

where $\xi_{nM}^\alpha(\rho_n) = \langle\rho_n|\xi_{nM}^\alpha\rangle$ is a solution of

$$(W_n^M + T_n^{\text{nuc}} + V_n^{\text{nuc}})|\xi_{nM}^\alpha\rangle = \epsilon_M^\alpha|\xi_{nM}^\alpha\rangle, \tag{4}$$

with eigenenergy ϵ_M^α and where the index α refers to a vibrational level in the electronic state M.

The intensity of a dipole transition from the vibronic state $|\phi_n^g\xi_{ng}^\alpha\rangle$ to the vibronic state $|\phi_n^e\xi_{ne}^\alpha\rangle$ is proportional to the squared magnitude of the transition dipole moment,

$$\langle\xi_{ng}^\alpha|\langle\phi_n^g|\vec{\mu}_n|\phi_n^e\rangle|\xi_{ne}^\beta\rangle, \tag{5}$$

where $\vec{\mu}_n$ is the electronic dipole operator of monomer n, which we will assume to be independent of nuclear coordinates, so that Eq. (5) can be written as

$$\langle\xi_{ng}^\alpha|\langle\phi_n^g|\vec{\mu}_n|\phi_n^e\rangle|\xi_{ne}^\beta\rangle = \langle\vec{\mu}_n\rangle f_\alpha^\beta, \tag{6}$$

with the abbreviation $\langle\vec{\mu}_n\rangle = \langle\phi_n^g|\vec{\mu}_n|\phi_n^e\rangle$ and where

$$f_\alpha^\beta = \langle\xi_{ng}^\alpha|\xi_{ne}^\beta\rangle \tag{7}$$

denotes the FC factor for a transition from the vibrational state α of the ground electronic state to the vibrational state β of the electronic excited state. With this notation the cross section for absorption out of the vibronic ground state $|\phi_n^g\xi_{ng}^0\rangle$ is given by

$$\sigma_M(E) \propto \sum_\beta |f_0^\beta|^2\delta(E - (\epsilon_e^\beta - \epsilon_g^0)), \tag{8}$$

where constant factors are omitted and $E=\hbar\omega$ is the energy of the photon.

B. The dimer: Basic formulas

The Hamilton operator of the dimer is

$$H = H_1(r_1,\rho_1) + H_2(r_2,\rho_2) + J(r_1,r_2), \tag{9}$$

where H_1, H_2 are the monomer Hamiltonians defined in Eq. (1) and $J(r_1,r_2)$ is the electronic dipole-dipole coupling matrix element. Since the two monomers are identical, the dimer Hamilton operator (9) remains unchanged under an exchange of the monomer indices. As we will see, this symmetry allows a considerable simplification of the dimer problem.

The vibronic ground state of the dimer is

$$|\psi_g^{00}\rangle = |\phi_1^g\xi_{1g}^0\rangle|\phi_2^g\xi_{2g}^0\rangle \tag{10}$$

with energy $E_g^{00} = \epsilon_g^0 + \epsilon_g^0$.

Remembering the exchange symmetry of the Hamiltonian (9) and denoting by P_{12} the operator that exchanges the monomer indices we define vibronic dimer states

$$|\psi_\pm^{\alpha\beta}\rangle = \frac{1}{\sqrt{2}}(|\phi_1^g\xi_{1e}^\alpha\rangle|\phi_2^g\xi_{2g}^\beta\rangle \pm |\phi_1^g\xi_{1g}^\beta\rangle|\phi_2^e\xi_{2e}^\alpha\rangle) \tag{11}$$

$$\equiv \frac{1}{\sqrt{2}}(|\pi_1^{\alpha\beta}\rangle \pm P_{12}|\pi_1^{\alpha\beta}\rangle) \tag{12}$$

and expand an arbitrary excited dimer state $|\psi^l\rangle$ with quantum number l as

$$|\psi^l\rangle = \sum_{\alpha\beta} (b_{l+}^{\alpha\beta}|\psi_+^{\alpha\beta}\rangle + b_{l-}^{\alpha\beta}|\psi_-^{\alpha\beta}\rangle). \tag{13}$$

Then projecting the eigenvalue equation

$$H|\psi^l\rangle = E_l|\psi^l\rangle \tag{14}$$

with H given by Eq. (9) onto states $\langle\psi_\pm^{\alpha\beta}|$ leads to a system of two *uncoupled* equations for the expansion coefficients $b_\pm^{\alpha\beta}$:

$$(\epsilon_e^\alpha + \epsilon_g^\beta)b_{l+}^{\alpha\beta} + J\sum_{\alpha'\beta'} f_{\alpha'}^\alpha f_\beta^{\beta'} b_{l+}^{\alpha'\beta'} = E_l b_{l+}^{\alpha\beta}, \tag{15}$$
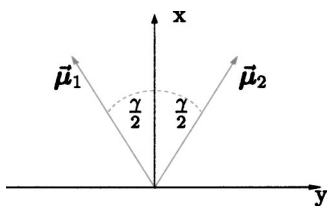
FIG. 1. Sketch of the orientation of the transition dipoles in the coordinate system used.

$$(\epsilon_e^\alpha + \epsilon_g^\beta)b_{l-}^{\alpha\beta} - J \sum_{\alpha'\beta'} f_{\alpha'}^\alpha f_{\beta}^{\beta'} b_{l-}^{\alpha'\beta'} = E_l b_{l-}^{\alpha\beta}. \tag{16}$$

Hence, the eigenstates can be classified by $\pm$ symmetry, i.e.,

$$|\psi_\pm^l\rangle = \sum_{\alpha\beta} b_{l\pm}^{\alpha\beta} |\psi_\pm^{\alpha\beta}\rangle. \tag{17}$$

Then, in principle, once the vibrational eigenenergies and states are known for an arbitrary form of the BO potentials, the systems (15) and (16) can be solved numerically. Solutions to the Eqs. (15) or (16) will be called $(+)$ or $(-)$ states, respectively. It is easy to see that solutions of the $(+)$ Eq. (15) for a given J are solutions of the $(-)$ equation for $-J$. If we are looking at energy levels and absorption into these levels as functions of J, then it is enough to do the calculations for the $(+)$ symmetry. This $\pm$ symmetry is valid only for identical monomers.

With knowledge of the dimer eigenenergies and eigenfunctions we are also able to calculate the absorption cross section for an incoming plane wave, whose electric part is given by $\vec{\varepsilon} = \hat{\varepsilon}\varepsilon \cos(\vec{k}\cdot\vec{r} - \omega t)$ (ε denotes the amplitude, $\hat{\mathcal{E}}$ the polarization vector, $\vec{k}$ the wave vector, and ω the frequency). In first-order perturbation theory, the cross section for absorption out of the vibronic ground state $|\psi_g^{00}\rangle$ with energy E_g^{00} is given in dipole approximation by

$$\sigma(\omega) \propto \sum_{\nu=\pm} \sum_l |\hat{\mathcal{E}} \cdot \langle \psi_\nu^l | \vec{\mu}_1 + \vec{\mu}_2 | \psi_g^{00}\rangle|^2 \delta(E_\nu^l - E_g^{00} - \hbar\omega). \tag{18}$$

If we use the expansion equation (17) we find

$$|\hat{\mathcal{E}} \cdot \langle \psi_\pm^l | \vec{\mu}_1 + \vec{\mu}_2 | \psi_g^{00}\rangle|^2 = \frac{1}{2}|\hat{\mathcal{E}} \cdot (\langle\vec{\mu}_1\rangle \pm \langle\vec{\mu}_2\rangle)|^2 \cdot \left|\sum_\alpha b_{l\pm}^{\alpha 0} f_0^\alpha\right|^2. \tag{19}$$

This expression consists of an "absorption strength" $|\sum_\alpha b_{l\pm}^{\alpha 0} f_0^\alpha|^2$ that is not explicitly dependent on the orientations of the monomer transition dipoles. However, it is dependent on the coupling strength J and therefore implicitly depends on the dimer geometry. To examine the remaining factor in Eq. (19), which does depend explicitly on the orientation of the transition dipole moments, we will use a coordinate system with the x-y-plane spanned by the two dipole transition moments $\vec{\mu}_1$ and $\vec{\mu}_2$ at an angle γ as shown in Fig. 1. For light polarized in the $\hat{x}$ direction we obtain for the geometry-dependent part of Eq. (19)

$$|\hat{x} \cdot (\langle\vec{\mu}_1\rangle \pm \langle\vec{\mu}_2\rangle)|^2 = \begin{cases} 2\mu^2(1 + \cos\gamma) \\ 0 \end{cases} \tag{20}$$

and for light polarized in the $\hat{y}$ direction

$$|\hat{y} \cdot (\langle\vec{\mu}_1\rangle \pm \langle\vec{\mu}_2\rangle)|^2 = \begin{cases} 0 \\ 2\mu^2(1 - \cos\gamma). \end{cases} \tag{21}$$

This means that for light polarized in the $\hat{x}$ direction, only $(+)$ levels and for light polarized in the $\hat{y}$ direction, only $(-)$ levels absorb. For unpolarized light the relative weight of absorption into the $(+)$ levels compared to absorption into the $(-)$ levels is dependent on the angle γ and is given by

$$\frac{(1 + \cos\gamma)}{(1 - \cos\gamma)}. \tag{22}$$

In the case of parallel transition dipole moments $(\gamma = 0°)$ only $(+)$ levels and in the case of antiparallel alignment $(\gamma = 180°)$ only $(-)$ levels absorb.

C. The vibrationless case

It is illustrative to present upper state eigenenergies as a function of the coupling strength J. The way in which this eigenspectrum changes with increasing complexity of the vibrational monomer spectrum will now be illustrated.

The simplest case is that of no vibrations at all, i.e., a single vertical transition energy. Taking $\epsilon_g^0 = 0$, the solutions of the Eqs. (15) and (16) are

$$E_\pm = \epsilon_e^0 \pm J. \tag{23}$$

Hence in the vibrationless case the two dimer levels are split linearly as J increases.

D. The case of *n* vibrational levels in the upper state

Initially we restrict the ground electronic state to its zero-point vibration and allow for n vibrational levels in the upper state. The dimer spectra are shown in Figs. 2(a)–2(c), where only the $(+)$ series of levels is plotted. As J increases each vibrational level splits linearly proportional to the square of its FC factor. The outermost levels split linearly with J in the strong-coupling limit whilst all other levels converge to intermediate values independent of J. In Fig. 2(c), where we have eight vibrational levels with Poisson distributed FC factors, one recognizes that the outermost negative energy level is continued "diabatically" through a sequence of ever-narrower avoided crossings to connect with the outermost positive-energy level. This means that as J becomes large the whole vibrational band on each monomer acts essentially as a single level whereas at small J each vibrational level interacts only with its degenerate partner on the other monomer.

The above behavior is confirmed by an examination of the absorption strength. For many vibrational levels in the upper electronic state the correlation between the distribution of oscillator strength and the avoided crossings in energy levels becomes evident. The case for three upper vibrational levels is shown in the right part of Fig. 2(a). For increasing negative J, oscillator strength disappears out of the upper two levels and is transferred to E_{0+}, exactly as in the two
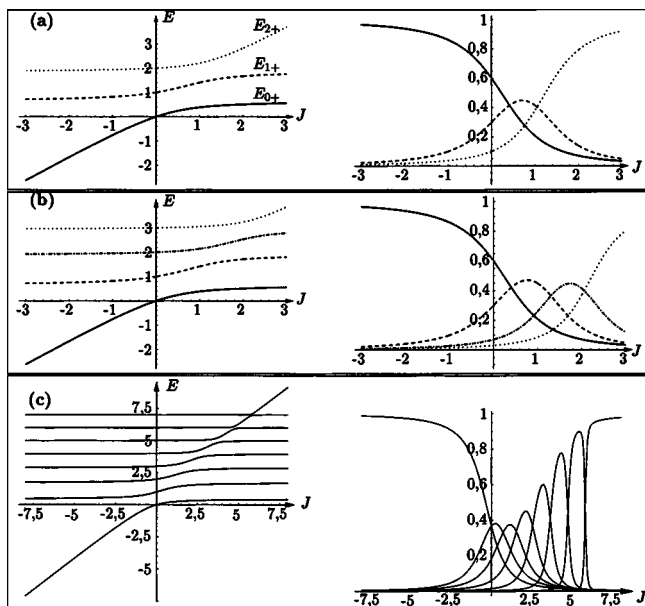
FIG. 2. Dimer eigenenergies (left figures) and absorption strength (right figures) for *n* vibration levels in the monomer upper electronic state. (a) Three levels, (b) four levels, and (c) eight levels.

vibrational level case. For positive J, the strength in E_{0+} decreases monotonically and that in E_{2+} increases monotonically to 100%. However, the level E_{1+} first experiences an increase in absorption strength and then a decrease, as J increases. The maximum occurs near to the position of the avoided crossing with E_{2+}, indicating a transfer of oscillator strength to the next higher level at this point. This pattern is repeated in Fig. 2(b) and 2(c) for four and eight upper vibrational levels, respectively. At each avoided crossing more and more of the oscillator strength is transferred "upwards" to appear ultimately 100% in E_{n+}. By contrast, for negative J, E_{0+} monotonically acquires all the oscillator strength and all other levels have diminishing strength as $|J|$ increases. Again one sees that for $|J|$ much greater than the vibrational bandwidth, the strong coupling limit oscillator strength appears in a single "diabatic" level corresponding to the vibrationless upper electronic dimer level. This behavior is reminiscent of a cooperative interaction between the levels of the vibrational band, leading to transfer of all the oscillator strength into a single level, which splits away from the rest of the band as the coupling strength increases.

E. The general case

Until now we have restricted ourselves to only one vibrational level in the electronic ground state. In the following we will increase the number of levels in the electronic ground state and examine how the energy spectrum changes. To establish a connection with the harmonic case which will be considered in much detail in the following section, we make the assumption that the potential energy surfaces for vibrational motion in the monomer electronic ground and in the excited electronic state are harmonic and the potential wells are identical but their minima separated by an amount $\Delta\rho$. Again we will take the zero of energy to be the zero-point vibration in the upper electronic state, an amount ΔE

above the corresponding level in the ground electronic state. If $\hbar\omega$ denotes the energy difference between successive energy eigenstates of these potentials then the energies in the electronic excited states are given by $\epsilon_e^n = n\hbar\omega$ and those of the electronic ground state are $\epsilon_g^n = n\hbar\omega - \Delta E$. The FC factors can be evaluated analytically and the monomer cross section for absorption out of the vibrational ground state of the electronic ground state is proportional to a Poisson distribution,[10]

$$\sigma_M(E) \propto \sum_n \frac{a^n}{n!} e^{-a} \delta(E - n\hbar\omega), \tag{24}$$

with $a = \omega\Delta\rho^2/(2\hbar)$. To compare with calculations of the following section we choose $a=1$. In the following we consider eight vibrational levels in the excited state (this is sufficient for convergence of the results), and vary the number of levels in the electronic ground state.

Since we have chosen the BO potentials in the ground and excited electronic states to be the same, for vanishing interaction J there occurs a degeneracy of the energy levels. This degeneracy, which is split for finite $|J|$, can be understood by examining Eq. (15) for $J=0$. All eigenenergies are given by

$$\epsilon_e^\alpha + \epsilon_g^\beta = (\alpha + \beta)\hbar\omega - \Delta E. \tag{25}$$

Here α can take the values $\alpha=0,\dots,\nu_e-1$ and $\beta=0,\dots,\nu_g-1$, where ν_e and ν_g are the number of vibrational levels in the electronic excited state and the electronic ground state, respectively.

In Fig. 3(a) the case of two vibrational levels in the electronic ground state is shown. For $J=0$ all states but the lowest and highest are twofold degenerate. If we compare the behaviour of the lowest energy level in Fig. 3(a) with the corresponding level in Fig. 2(c), we see that for strong negative coupling both have positive gradient but for strong positive coupling in the case with just one vibrational level in the electronic ground state the gradient is zero, whereas in the case of two levels it has a negative gradient. For both positive and negative coupling there are diabatic levels that are continued through sequences of avoided crossings. In Fig. 2(c) all levels but the lowest have zero gradient in the case of strong negative coupling. However in Fig. 3(a) also the second lowest level pair, which are degenerate for $J=0$, has a negative gradient. These levels are also continued diabatically into the positive J region, so that for large positive J three levels split off linearly from the band of remaining constant-energy levels. In the region between weak and strong coupling there appear again avoided crossings. To sum up, in the case of two vibrational levels in the ground electronic state we find three diabatic levels with positive gradient and one with negative gradient.

When three levels in the ground electronic state are considered [Fig. 3(b)] there results a similar change in the energy spectrum as in going from one to two states. Now there are levels that are threefold degenerate for $J=0$. Then we find six, (i.e., $1+2+3$) diabatic levels with positive gradient and three $(1+2)$ diabatic levels with negative gradient.

The last case we consider is that of six levels in the electronic ground state. Now the energy spectrum [Fig. 3(c)]
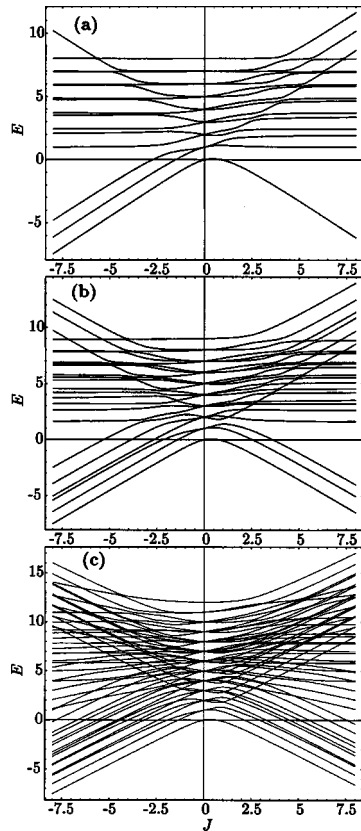
FIG. 3. Dimer energy levels in the harmonic model with eight vibrational levels in the electronic excited state and (a) two, (b) three, and (c) six vibrational levels in the ground state. The unit of energy is $\hbar\omega$.

looks very complicated, with a lot of avoided crossings. In the case of strong coupling there are still levels with zero gradient asymptotically. In the next section, using method (2), we will explain this spectrum in the case of an infinite number of levels in both the ground and excited electronic states in more detail and we will expose the origin of the crossings between energy eigenvalues as a function of coupling strength J.

III. THE JAYNES–CUMMINGS HAMILTONIAN

A. Derivation

In Sec. II we have traced the development of the dimer spectrum as the number of vibrational levels in the excited and ground electronic states increases. In this section an approximation is used that allows *all* vibrational levels of both excited and ground electronic states to be considered. However, to make the problem tractable the vibrational motion is assumed harmonic in both ground and excited electronic states. Then, as we will see below, the vibronic coupling is not mediated directly by the FC factors as in Sec. II but by a term linear in the normal coordinate, arising from the shift in equilibrium nuclear coordinate between ground and excited states. As the vibrations are harmonic such an approximation lends itself naturally to an expression in operator form. This also emphasizes the similarity of phonons and photons since the resulting problem is identical to the celebrated Jaynes–Cummings model of quantum optics,[9] in which a two-level atom interacts with the quantized photon field.

Considering that the monomer vibrational progression is due to the harmonic vibration of normal coordinates ρ_1 and ρ_2 of monomers 1 and 2, respectively, and that the frequency ω is the same in ground and excited electronic states, we have for the BO potentials for monomer n in ground and excited states

$$V_n^g = \tfrac{1}{2}\omega^2\rho_n^2, \tag{26}$$

$$V_n^e = \tfrac{1}{2}\omega^2\rho_n^2 - \omega^2\rho_n\Delta\rho_n + \widetilde{E}_n, \tag{27}$$

where $\Delta\rho_n$ is the shift in the potential minimum between ground and excited states and

$$\widetilde{E}_n = \tfrac{1}{2}\omega^2(\Delta\rho_n)^2 + \Delta E_n, \tag{28}$$

with ΔE_n being the shift in energy between the two potential minima. Thus the shifted upper state potential is equivalent to an unshifted potential with a linear term added. We define the vibronic coupling

$$g_n = \frac{\omega^{3/2}\Delta\rho_n}{\sqrt{2\hbar}}. \tag{29}$$

For identical monomers $g_1 = g_2 = g$ and $\widetilde{E}_1 = \widetilde{E}_2 = \widetilde{E}$. Recognizing that the two-level molecular system is isomorphic to the spin-$\tfrac{1}{2}$ system we introduce the Pauli spin operators:

$$\sigma_x = |\pi_1\rangle\langle\pi_2| + |\pi_2\rangle\langle\pi_1|, \tag{30}$$

$$\sigma_z = |\pi_1\rangle\langle\pi_1| - |\pi_2\rangle\langle\pi_2|. \tag{31}$$

Here $|\pi_1\rangle = |\phi_1^e\rangle|\phi_2^g\rangle$ and $|\pi_2\rangle = |\phi_1^g\rangle|\phi_2^e\rangle$. If c_1 and c_2 are boson operators for harmonic vibrations on monomers 1 and 2, respectively, we introduce the symmetrized boson operators,

$$c_r = \frac{1}{\sqrt{2}}(c_1 - c_2), \tag{32}$$

$$c_s = \frac{1}{\sqrt{2}}(c_1 + c_2), \tag{33}$$

then the excited state Hamiltonian of the dimer H_e can be written in the form

$$H_e = \left[J\sigma_x - \frac{\hbar g}{\sqrt{2}}(c_r^\dagger + c_r)\sigma_z + \hbar\omega c_r^\dagger c_r \right] + \left[\widetilde{E} - \hbar\omega c_s^\dagger c_s \right.$$
$$\left. - \left(\frac{\hbar g}{\sqrt{2}}\right)(c_s^\dagger + c_s) \right] \equiv H_{JC} + H_{OS}. \tag{34}$$

Several remarks are in order here. One notes that the dependence on c_r and c_s has separated. In first quantization these symmetry-adapted operators correspond to $\rho_r = \rho_1 - \rho_2$, the relative coordinate of internal vibration of two monomers and $\rho_s = \rho_1 + \rho_2$, the center-of-mass coordinate. Such a separation was already made in Refs. 1 and 2. The second term H_{OS} in the Hamiltonian, involving in-phase oscillation of the two monomers, is simple to diagonalize as a displaced harmonic oscillator. The first part H_{JC} is nontrivial involving the excitation transfer. The identity of H_{JC} with the JC model of quantum optics occurs since the coupling of the electromagnetic (EM) field to the atom in dipole approximation is also

linear and the EM field is purely harmonic, as in Eqs. (26) and (27).

The JC Hamiltonian has been the subject of much study[8] in quantum optics and in problems of solid-state physics where a spin-$\frac{1}{2}$ system is coupled linearly to a bosonic field. Its applicability to the dimer problem can be questioned since the harmonic oscillator, with an infinite number of vibrational levels is not a good approximation to the monomer vibrational degree of freedom which is better described by a finite number of anharmonic levels. Nevertheless, if we restrict discussion to relatively low levels of vibrational excitation, where the approximation is reasonable, this ubiquitous Hamiltonian H_{JC} is useful to study in the dimer context, since it readily lends itself to solution in an adiabatic approximation, as discussed in detail below.

With the centre-of-mass motion solved trivially we will concentrate on H_{JC} and drop the subscript "r," i.e.,

$$H_{JC} = \hbar\omega c^\dagger c - \frac{\hbar g}{\sqrt{2}}(c^\dagger + c)\sigma_z + J\sigma_x. \tag{35}$$

First we note that if there are no vibrations, there remains the electronic Hamiltonian

$$H^{el} = J\sigma_x = J(|\pi_1\rangle\langle\pi_2| + |\pi_2\rangle\langle\pi_1|). \tag{36}$$

The eigenstates are of the form [cf. Eq. (12)]

$$|\pi_\pm\rangle = \frac{1}{\sqrt{2}}(|\pi_1\rangle \pm |\pi_2\rangle) \tag{37}$$

with eigenenergies

$$E_\pm = \pm J. \tag{38}$$

This is identical with Eq. (23) when we take the monomer excitation energy ϵ_e^0 to define the zero of energy.

The eigenstates (37) are eigenstates of the operator σ_x with eigenvalues ± 1 and therefore in the vibrationless case σ_x is identical to the exchange operator P_{12}, which exchanges the monomer indices [see Eq. (12)]. This fundamental symmetry of the symmetric dimer is preserved when vibrations are considered. Then however, the exchange operator involves also the parity of vibrations, i.e.,

$$P_{12} = \mathcal{P}\sigma_x = e^{i\pi c^\dagger c}\sigma_x, \tag{39}$$

where $\mathcal{P}$ is the parity operator

$$\mathcal{P}\rho_r = \mathcal{P}(\rho_1 - \rho_2) = -\rho_r = (\rho_2 - \rho_1). \tag{40}$$

Therefore $\mathcal{P}$ functions also as the exchange operator in the space of vibrations, hence the form (39). In Ref. 8 this operator is given in the equivalent form $\exp[i\pi(c^+c + \sigma_x + \frac{1}{2})]$.

It is not difficult to show that the operator P_{12} of Eq. (39) commutes with H_{JC} and has eigenvalues ± 1. Hence the whole spectrum separates into two branches and the eigenfunctions may be expanded as

$$|\psi_\pm\rangle = \frac{1}{\sqrt{2}}(|\chi_\pm\rangle|\pi_1\rangle \pm \mathcal{P}|\chi_\pm\rangle|\pi_2\rangle). \tag{41}$$

Note that here, in contrast to Eq. (11) and as is more appropriate in the harmonic case where the vibrational states have definite parity, we have separated the dimer vibrational states
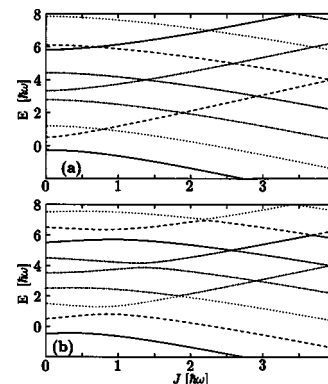

FIG. 4. Comparison of the adiabatic (a) with the exact (b) eigenvalues of the JC Hamiltonian as a function of the coupling strength J and with $g = \omega$. Only levels with positive eigenvalue of the operator P_{12} are plotted.

$|\chi_\pm\rangle$ from the purely electronic states $|\pi_n\rangle$. The vibrational states $|\chi_\pm\rangle$ are eigenstates of the symmetrized Hamiltonian,

$$H_{JC}^\pm = \hbar\omega c^\dagger c - \frac{\hbar g}{\sqrt{2}}(c^\dagger + c) \pm J\mathcal{P}, \tag{42}$$

i.e.,

$$H_{JC}^\pm|\chi_\pm\rangle = E_\pm^{JC}|\chi_\pm\rangle. \tag{43}$$

B. Solution of the JC problem

The Eq. (43) can be readily solved numerically by expanding the dimer vibrational states belonging to the relative coordinate ρ_r in the harmonic eigenfunctions $\xi^n(\rho_r)$ of the oscillator, i.e.,

$$|\chi_\pm\rangle = \sum_{n=0}^{N} a_n^\pm|\xi^n\rangle \tag{44}$$

leading to a matrix diagonalization for the eigenenergies $E_\pm^{JC}$ and coefficients $a_n^\pm$. Physically the dimension N for the oscillator problem is infinite. Practically we have limited N to ≈ 100 which ensures good convergence of the lower eigenvalues. We take the coupling parameter g as positive, as in a physical molecule, although mathematically the eigenvalues are invariant under a change of sign of g. The numerical results are presented in Fig. 4 below.

However, first it is instructive to consider an adiabatic approximation, in which the nuclear kinetic energy operator is neglected in zeroth order. This can be best derived by reverting to the coordinate picture for the vibration, i.e., we put

$$c = \frac{1}{\sqrt{2\hbar\omega}}(\omega q + ip), \tag{45}$$

$$c^\dagger = \frac{1}{\sqrt{2\hbar\omega}}(\omega q - ip) \tag{46}$$
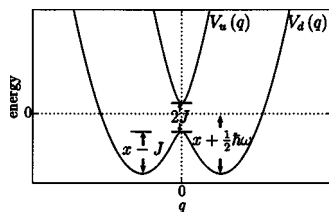
to give the JC Hamiltonian

FIG. 5. The adiabatic potentials of the JC Hamiltonian defined in Eq. (48). The parameter x is given by $J^2\omega/(2\hbar g^2)+\hbar g^2/(2\omega)$.

$$H_{JC} = \tfrac{1}{2}(p^2 + \omega^2 q^2) - \tfrac{1}{2}\hbar\omega - \sqrt{\hbar\omega}gq\sigma_z + J\sigma_x. \tag{47}$$

With neglect of $\tfrac{1}{2}p^2$, for fixed q one can diagonalise H_{JC} to give the two adiabatic potentials

$$V_{u,d}(q) = \tfrac{1}{2}\omega^2 q^2 - \tfrac{1}{2}\hbar\omega \pm \sqrt{(J^2 + \hbar\omega g^2 q^2)} \tag{48}$$

and correspondingly two sets of eigenenergies for each parity, given by the solutions of

$$(\tfrac{1}{2}p^2 + V_{u,d}(q))\chi_{u,d}^{\pm}(q) = E_{\pm}\chi_{u,d}^{\pm}(q). \tag{49}$$

For $\hbar g^2/\omega \gtrsim J$ the lower potential $V_d(q)$ shows a double-well structure and is much broader than the upper potential $V_u(q)$ as shown in Fig. 5.

The eigenenergies calculated in the adiabatic picture are shown in Fig. 4(a) and for comparison the exact results are juxtaposed in Fig. 4(b). One notes the avoided crossings between successive levels in the exact solution. However, compared to the case of a limited number of vibrational levels, as considered in Sec. II, in the case of an infinite number of harmonic levels the asymptotic behavior for large J is quite different. In this case asymptotically *each* vibrational level shifts linearly with $\pm J$. Thus, two parallel equidistant sets of levels are formed. Indeed one can show analytically that, in the limit of large J, for fixed n the energy levels are simply given by

$$E_{\pm}^{n} = n\hbar\omega \pm (-1)^n J. \tag{50}$$

As seen from Eq. (34) the dimer eigenenergies are a sum of those of the JC Hamiltonian and those of the shifted oscillator Hamiltonian H_{OS}. Hence, on each JC eigenenergy is built an infinite series of oscillator levels and each avoided crossing of the JC energies generates a whole series of avoided crossings in the full spectrum, giving the complicated picture shown in Fig. 6. One should note that in Fig. 6 just a small part of the J, E parameter space compared to Fig. 3(c) is shown.
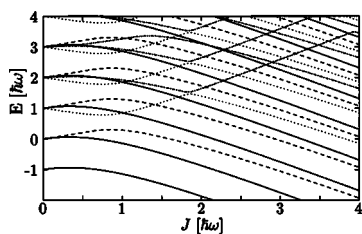

FIG. 6. The full dimer eigenvalues for positive exchange eigenvalue as a function of J with $g = \omega$.

C. The absorption spectrum

As in Sec. II we will calculate the photoabsorption spectrum for absorption out of the ground harmonic vibrational level of the monomer ground electronic state. As we have seen there, for a shifted harmonic oscillator in the excited electronic state, the FC factors follow a Poisson distribution and therefore the monomer "stick" spectrum is a sequence of equidistant peaks whose heights also follow a Poisson distribution, i.e., the monomer absorption cross section is given by

$$\sigma_M(E) \propto \sum_n \left[\frac{1}{n!}\left(\frac{g^2}{\omega^2}\right)^n \exp\left(-\frac{g^2}{\omega^2}\right) \right] \delta\left(E - n\hbar\omega + \frac{\hbar g^2}{\omega}\right). \tag{51}$$

Note, that due to our slightly different definition of the zero of energy the whole spectrum is shifted by an energy $\hbar g^2/\omega$ compared to the calculations in Sec. II.

The dimer energy spectrum, as explained in the previous section [see Eq. (34)], is a sum of the JC spectrum and the harmonic levels of the shifted oscillator. Since the initial state is unique, the absorption strength in each line is then given by a product of the square of the FC factor for absorption to the JC level multiplied by the Poisson distribution for absorption to the shifted oscillator levels. If $|\xi^0\rangle$ denotes the ground state of the harmonic oscillator belonging to the ρ_r coordinate and $|\chi_{\pm}^m\rangle$ is a solution of Eq. (43) then the dimer spectrum is

$$\sigma_D^{\pm}(E) \propto 2\sum_{m,n} |\langle\xi^0|\chi_{\pm}^m\rangle|^2 \left[\frac{1}{n!}\left(\frac{g^2}{2\omega^2}\right)^n \exp\left(-\frac{g^2}{2\omega^2}\right) \right]$$
$$\times \delta\left(E - E_{JC}^{m\pm} - n\hbar\omega + \frac{\hbar g^2}{2\omega}\right) \tag{52}$$

giving the absorption strength into the nth vibrational level built on the mth JC eigenvalue. Note that the shift of the dimer harmonic oscillator, describing the center-of-mass motion is a factor $\sqrt{2}$ larger than that of the monomer excited state potential.

For intermediate coupling the spectrum is very complicated corresponding to absorption into several JC levels. However for strong coupling, one JC level splits off and the spectrum is again Poissonian [Eq. (52) with only one JC eigenvalue contributing]. This behavior was demonstrated long ago[2,3,11] and indeed, in the harmonic approximation the energy and absorption spectra calculated in the JC formulation are identical with those of the diagonalization method of Sec. II. However, as we will now show, the adiabatic JC approximation affords a simple explanation of the apparently complicated spectral behavior.

From Fig. 4 one sees that the adiabatic levels provide the connection through the avoided crossings of the exact JC eigenvalues. Asymptotically for large J the avoided crossings become extremely narrow and the spectrum consists of two sets of levels increasing or decreasing in energy linearly with J. Hence the adiabatic energies are exact in the large J limit. From Fig. 5 one can see that the splitting between the two adiabatic potentials increases linearly with J, so that the levels with increasing energy as J increases are associated with the upper potential and those with decreasing energy with the
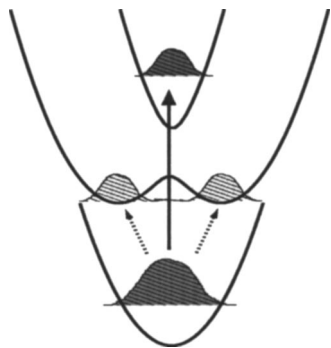
FIG. 7. Schematic representation of absorption from the dimer ground state to states of the adiabatic potentials.

FIG. 8. The dimer spectrum for various damping times τ calculated from Eq. (53).

lower potential. The two sets of levels show real crossings for small J, i.e., levels of the lower potential are degenerate with those of upper potential. When nonadiabatic couplings are taken into account, as in the exact results of Fig. 4(b), their crossings are avoided. In this way the adiabatic approximation yields a simple interpretation of the behavior of the exact eigenenergies as a function of J.

Hence one can associate the adiabatic curves with an imaginary continuous connection of the avoided crossings of Fig. 2(c), giving a state increasing linearly with J. In this figure, it was also shown that this state carries successively more of the oscillator strength as J increases. By explicit calculation we have shown that, as in Fig. 2(c), the oscillator strength for absorption is also transferred successively at the avoided crossings of Fig. 5(b) and that the lowest linearly increasing adiabatic curve has oscillator strength which follows the locus of the maxima of curves similar to those of Fig. 2(c). Indeed the adiabatic picture illustrates nicely the origin of this transfer of oscillator strength. As sketched in Fig. 7 it is plausible that the dominant absorption from the ground state of the dimer is to the ground state of the upper adiabatic potential well V_u since they have maximum overlap. The latter state can be identified with the lowest adiabatic state whose energy increases linearly with J. The avoided crossings in the exact results are caused by states of the lower adiabatic potential become degenerate, and therefore mixing, with this state. As J increases, successively higher-lying states of the lower potential pass through the ground state of the upper potential and acquire its oscillator strength. In the limit of large J the ground state and upper state adiabatic potential wells become identical in shape [see Eq. (48)], so that the zero-zero transition of Fig. 7 does carry almost 100% of the oscillator strength, giving in the full spectrum a single Poisson sequence.

IV. TIME-DEPENDENT CALCULATION OF DIMER SPECTRA

In this section the absorption spectrum will be calculated from the long-time limit of the dimer wave functions propagated numerically in time. The absorption cross section (18) can be written as[12–14]
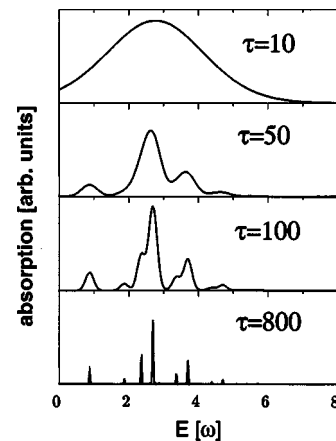
$$\sigma(\omega) \sim \int_{-\infty}^{\infty} dt\, e^{i(E_g^{00}+\hbar\omega)t/\hbar} c(t), \qquad (53)$$

where the time-correlation function $c(t)$ is given as

$$c(t) = \hat{\boldsymbol{\mathcal{E}}} \cdot \langle \psi_g^{00}\vec{\boldsymbol{\mu}}|U_e(t)|\vec{\boldsymbol{\mu}}\psi_g^{00}\rangle \cdot \hat{\boldsymbol{\mathcal{E}}}. \qquad (54)$$

Here $\vec{\boldsymbol{\mu}} = \vec{\boldsymbol{\mu}}_1 + \vec{\boldsymbol{\mu}}_2$ is the electronic dipole operator of the dimer and $U_e(t)$ denotes the propagator $U(t) = e^{-iH_e t/\hbar}$ containing the excited state Hamiltonian H_e of the system. We now calculate the correlation function starting from the ground state nuclear wave function $\xi_g^{00}(\rho_1,\rho_2)$ $= \xi_{1g}^0(\rho_1)\xi_{2g}^0(\rho_2)$. Then, introducing complete sets of electronic states, the time-correlation function (54) becomes

$$c(t) = \sum_{n,m=1}^{2} \hat{\boldsymbol{\mathcal{E}}} \cdot \langle \vec{\boldsymbol{\mu}}_n\rangle \langle \pi_n|\langle \xi_g^{00}|U_e(t)|\xi_g^{00}\rangle|\pi_m\rangle \langle \vec{\boldsymbol{\mu}}_m\rangle \cdot \hat{\boldsymbol{\mathcal{E}}}, \quad (55)$$

which upon Fourier transformation from time to frequency domain (53), yields the spectrum. The calculation of the correlation function requires the time propagation of the initial wave function on the coupled BO potentials of the electronically excited states. In our numerical application the wave functions are represented on a grid, sampling the two coordinates ρ_1, ρ_2. The time propagation is performed with the method of Feit and Fleck[15] and the off-diagonal coupling is treated as is described in Ref. 16.

Although our numerical method is neither limited to harmonic potentials nor to constant coupling J, we here employ the same harmonic potentials [given by Eqs. (26) and (27)] and a constant coupling, as used in the preceding sections. Figure 8 shows dimer spectra calculated using the time dependent approach. The curves were obtained for $\omega = J = 0.2$, and only the $(+)$ band is displayed. The energy is given in units of ω and the normalization is such that the excited state potential surface has its minimum at zero energy. The four panels in the figure represent cases of different experimental resolution. In calculating the spectra via Eq. (53), the correlation function $c(t)$ is multiplied by a Gaussian damping function $g(t) = \exp[-4\,ln(2)(t/\tau)^2]$, where the damping time τ (in atomic units) denotes the full width at half maximum. With increasing width of the damping function, see Fig. 8, the structureless absorption band exhibits a vibrational fine
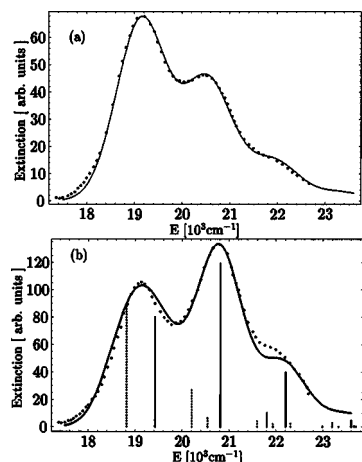
FIG. 9. Comparison of theory and experiment in the case of Dye1. (a) Monomer extinction coefficient. (b) Dimer extinction coefficient, measured (dots), and fitted (continuous line). The vertical lines are the undressed stick spectra; solid, $(+)$ symmetry and dashed, $(-)$ symmetry.

FIG. 11. Same as Fig. 9 but for Dye3.

structure which, in the limit of infinite times, leads to δ peaks as obtained from the time independent calculation. In fact the spectrum of Fig. 8 for $\tau=800$ is in perfect agreement with the results of method (1).

Since in many experiments vibrational bands are not determined with high resolution (see Sec. V), the time dependent approach has the advantage that such diffuse bands can be obtained via a short-time propagation. In other words, within the time-independent approach the stick spectrum is calculated and afterwards broadened to make contact with experiment. The wave packet calculation, on the other hand, can be stopped after a relatively short propagation time to yield a low resolution spectrum.[17] This is advantageous in going to larger systems since it is possible to replace exact wave packet propagation techniques by approximate methods adequate for short times.

V. COMPARISON WITH EXPERIMENT

In this section we will compare the theories with experiment. To this end we have chosen three examples of measured dimer spectra from the literature. The first one
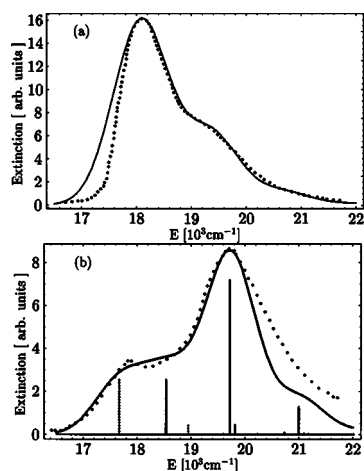
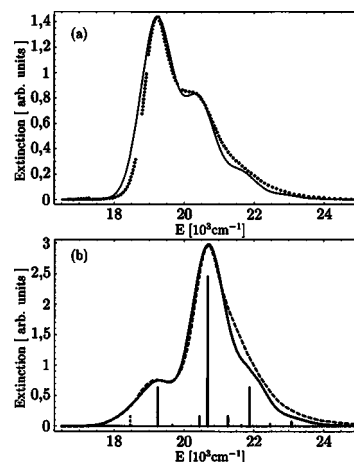is the famous dye molecule pseudoisocyanine (Dye 1) already treated successfully by Kopainsky, Hallermeier, and Kaiser[18] using the theory of Merrifield and Fulton and Gouterman. The second example is an old measurement of West and Pearce[19] on 3,3′-diethylthiacarbocyanine p-toluenesulphonate (Dye 2). Finally we investigate a very recent experiment by Baraldi *et al.*[20] on 3,3′-disulfopropyl-4,5, 4′,5′-dibenzo-9-ethyloxacarbocyanine (Dye 3), for recent work on merocyanine dimers see Ref. 21. The corresponding monomer and dimer absorption spectra are shown in Figs. 9–11. All of these spectra show considerably broadened lines due to finite temperature and interaction with the solvent molecules, whereas the theory of the previous sections provides only stick spectra. Therefore we "dress" the stick spectra with a line shape function which we have chosen to be Gaussian. With this broadening the monomer spectra can be fitted quite well by a Poisson distribution. In the case of Dye1 [Fig. 9(a)] the fit is almost perfect. For the other two dyes the agreement is not so good but the assumption of a Poisson distribution seems still reasonable and is necessary to apply the harmonic theory of the previous sections.

The fits provide the monomer parameters ω_{00} (the position of the lowest vibrational peak), ω (the vibrational frequency), and g (the vibrational coupling strength) which we use as input for our calculations. The parameters obtained in this way are given in Table I together with the width of the convoluted Gaussian σ_M.

For the calculations of the dimer absorption spectra we used as parameter the coupling strength J and, since the ge-

FIG. 10. Same as Fig. 9 but for Dye2.

TABLE I. The parameters used to obtain the spectra of Figs. 9–11.

	Dye1	Dye2	Dye3
ω_{00} (cm^{-1})	19130	18070	19200
ω (cm^{-1})	1390	1280	1200
g/ω	0.78	0.60	0.72
σ_M (cm^{-1})	520	500	450
$J/\hbar\omega$	0.46	0.65	0.77
γ	69°	55°	28°
$\Delta E_D/\hbar$ (cm^{-1})	140	300	0
σ_D (cm^{-1})	460	460	450

ometry of the dimers is not known, the angle γ between the two dipole transition moments. The stick spectra are shifted by an amount ΔE_D and then convoluted with a Gaussian line shape function of width σ_D. The spectra obtained are shown in Fig. 9–11 together with the underlying stick spectra for the $(+)$ and $(-)$ symmetry. The corresponding fit parameters can also be found in Table I. All calculated dimer spectra are in good agreement with the measured ones. For Dye1 and Dye2 we had to introduce a quite large shift ΔE_D, but no shift was needed in the case of Dye3. The values of the coupling strength J indicate intermediate coupling which is the most severe test of theory.

Baraldi *et al.*[20] made comprehensive theoretical investigations on Dye3 using molecular dynamics and Monte Carlo calculations of the dimer structure and comparative analysis of monomer and dimer spectra. They concluded that the planes of monomers in the dimer are parallel but the axes are not parallel, rather they are twisted to an angle of about 30°. This value is close to the value of $\gamma = 28°$ obtained from the fit of Fig. 11. One should note that in this figure both peaks, at $\sim 19\,000$ and $\sim 21\,000$ cm^{-1}, come from the $(+)$ band. The $(-)$ band was just needed to fit the low energy tail properly.

VI. CONCLUSIONS

In this paper we have considered three quite separate methods for the calculation of dimer spectra. The first method is derived in first quantization and involves a direct diagonalization of the vibronic coupling problem, in which the input consists of energies of vibrational levels in ground and excited electronic states and the FC factors between them. This has the advantage that it is applicable to arbitrary BO potentials. For example, if the potentials are known from quantum chemistry calculations, eigenenergies and FC factors are calculated easily. Alternatively, experimental monomer spectra may be fitted to derive the necessary data.

The second method, more suited to the harmonic approximation, proceeds by separation of an operator equation identical to the JC equation of quantum optics, namely, that describing a two-level system interacting with a quantized bosonic oscillator field. Apart from this interesting connection the method readily lends itself to an adiabatic approximation which allows a more physical interpretation to be given to the spectral changes, both in energy levels and oscillator strength, accompanying the transition from the weak-coupling to the strong-coupling regimes.

One general aspect to emerge from these studies is that the energy spectrum as a function of coupling strength J depends crucially upon the number of bound vibrational states supported by the ground-state BO potential. If only one state is considered, as in Fig. 2, a single quasiadiabatic state shifts linearly with J but all other levels have constant energy as J becomes large. However as the number of levels in the electronic ground-state increases, e.g., in Fig. 3, more and more dimer levels behave linearly, presumably due to level repulsion. In the harmonic limit of an infinite number of ground-state vibrational levels, all dimer energies change linearly with J, see Eq. (50). Since realistic molecules have a finite number of bound levels, it is expected that the precise details of dimer spectra will be specific to each monomer.

The third method is different to these studies and involves a direct time propagation of nuclear degrees of freedom on coupled BO surfaces. For times long compared to vibrational periods, spectra are obtained which are in complete agreement with those of the diagonalization method provided that in the latter method a sufficient number of vibrational levels are used to assure convergence for a given value of J. The time-dependent method has the advantage that it can also be used to study transient processes, e.g., in femtosecond chemistry.

Dimer spectra calculated using these methods show excellent agreement with experiment as to the changes in shape of the vibrational envelope with respect to that of the monomer. In these calculations the monomer spectra are used as input in the harmonic approximation and the coupling strength J is used as a fit parameter since it is not known independently. Then the complete shape of the measured dimer spectra are predicted correctly even in the intermediate coupling case. In principle the values of J obtained from the fits could be used to throw light on the dimer geometry, since our fits indicate a specific orientation angle of transition dipoles. Although detailed spectral shapes are in good agreement with experiment, in two cases it is necessary to shift the whole calculated spectrum by a constant amount to bring in agreement with the measured spectrum. Although we did not investigate the origin of this shift further it could also give information on the changes in molecule-solvent interaction accompanying dimerization.

[1] A. Witkowski and W. Moffitt, J. Chem. Phys. **33**, 872 (1960).
[2] R. E. Merrifield, Radiat. Res. **20**, 154 (1963).
[3] R. L. Fulton and M. Gouterman, J. Chem. Phys. **41**, 2280 (1964).
[4] M. J. Riley and E. R. Krausz, Chem. Phys. **148**, 229 (1990).
[5] M. Sonnek, H. Eiermann, and M. Wagner, Phys. Rev. B **51**, 905 (1995).
[6] C. Koch and B. Esser, J. Lumin. **81**, 171 (1999).
[7] W. T. Simpson and D. L. Peterson, J. Chem. Phys. **26**, 588 (1957).
[8] R. Graham and M. Höhnerbach, Z. Phys. B: Condens. Matter **57**, 233 (1984).
[9] E. T. Jaynes and F. W. Cummings, Proc. IEEE **51**, 89 (1963).
[10] E. S. Medvedev and V. I. Osherov, *Radiationless Transitions in Polyatomic Molecules* (Springer, Berlin, 1995).
[11] J. S. Briggs and A. Herzenberg, Mol. Phys. **23**, 203 (1972).
[12] M. Lax, J. Chem. Phys. **20**, 1752 (1952).
[13] R. G. Gordon, Adv. Magn. Reson. **3**, 1 (1968).
[14] E. J. Heller, Acc. Chem. Res. **14**, 368 (1981).
[15] M. D. Feit, J. A. Fleck, and A. Steiger, J. Comput. Phys. **47**, 412 (1982).
[16] J. Alvarellos and H. Metiu, J. Chem. Phys. **88**, 4957 (1988).
[17] V. Engel, R. Schinke, S. Hennig, and H. Metiu, J. Chem. Phys. **92**, 1 (1990).
[18] B. Kopainsky, J. Hallermeier, and W. Kaiser, Chem. Phys. Lett. **83**, 498 (1981).
[19] W. West and S. Pearce, J. Phys. Chem. **69**, 1894 (1965).
[20] I. Baraldi, M. Caselli, F. Momicchioli, G. Ponterini, and D. Vanossi, Chem. Phys. **275**, 149 (2002).
[21] F. Würthner, S. Yao, T. Debaerdemaeker, and R. Wortmann, J. Am. Chem. Soc. **124**, 9431 (2002).